J. Math. Computer Sci., 38 (2025), 396–416

Online: ISSN 2008-949X

Journal of Mathematics and Computer Science

Journal Homepage: www.isr-publications.com/jmcs

On nonlinear dynamics in a fractional order model for antibiotic resistance

Abdelalim A. Elsadany[a,b,*], Amr Elsonbaty[a,c]

[a]Department of Mathematics, College of Science and Humanities in Al-Kharj, Prince Sattam bin Abdulaziz University, Al-Kharj, 11942, Saudi Arabia.

[b]Department of Basic Science, Faculty of Computers and Informatics, Suez Canal University, Ismailia 41522, Egypt.

[c]Department of Engineering Mathematics and Physics, Faculty of Engineering, Mansoura University, Mansoura 35516, Egypt.

Abstract

This study presents a fractional-order mathematical model to address the pressing issue of global antibiotic resistance. The focus is to delve into the nonlinear dynamics of this model and comprehensively analyze the impacts of crucial factors and parameters. Our investigation includes exploring the existence, uniqueness, and positivity of the solution. We identify the equilibrium points of the model and analyze their stability. To explore the effects of parameters on the model's dynamics, we obtain stability regions, time series solutions, and phase diagrams. Numerical simulations, using the Adams-Bashforth-Moulton method, are conducted to validate the theoretical analysis results.

Keywords: Antibiotic resistance, equilibrium points, local stability, global stability, Caputo fractional derivative.

2020 MSC: 34A08, 34D05, 97M60, 37M05.

1. Introduction

In 2019, the World Health Organization declared ten threats as the most influential to human health. These threats include global influenza pandemics, noncommunicable diseases, antibiotic resistance, ebola, and other high-threat pathogens [42]. Indeed, antibiotics have been successfully used for a long time as effective medical treatments for a plethora of human infections as well as the control of dangerous human diseases. For example, antibiotics enable us to easily treat infections like pneumonia, tuberculosis, gonorrhea, and salmonellosis, which were not possible in the past. Antibiotics are also extensively used in agriculture and food production, animal farming, and medical procedures against animal epidemic outbreaks.

Over time, bacteria have unfortunately developed antibiotic resistance. There are several factors contributing to this concerning phenomenon [17, 20, 25, 42]. First and foremost, bacteria naturally acquire resistance during their replication process. Additionally, the misuse of antibiotics in both humans and animals is accelerating the development of antibiotic resistance. This misuse includes inappropriate prescribing, overuse, and improper administration of antibiotics. Furthermore, there is a lack of sufficient

*Corresponding author
Email address: aelsadany1@yahoo.com (Abdelalim A. Elsadany)

doi: 10.22436/jmcs.038.03.08

Received: 2024-06-09 *Revised:* 2024-11-25 *Accepted:* 2024-12-12

investment in both hospital infection control and scientific research aimed at discovering new types of antibiotics. This hinders progress in combating antibiotic resistance effectively. Compounding the issue is the absence of crucial governmental regulations on medical facilities in certain regions of the world. This lack of oversight allows for inadequate control measures and contributes to the proliferation of antibiotic resistance. Lastly, pollution, in various forms, plays a strong role in increasing the development of antibiotic resistance. The release of antibiotics and resistant bacteria into the environment through wastewater, agricultural practices, and other sources contributes to the spread and persistence of antibiotic resistance. Antibiotic resistance refers to the observed ability of some bacteria, viruses, fungi, and parasites to resist antibiotics/antiviral medical treatments. Antibiotic resistance is driven by the overuse of antibiotic in people and animals. The possible consequences of this threat include the reappearance of some diseases that were thought to have disappeared, in addition to seriously compromising medical surgeries and chemo-therapies. Another example is the resistance to tuberculosis drugs, which causes around 10 million infections and 1.3 million deaths every year [2].

Antibiotic resistance is a growing public health crisis characterized by the ability of bacteria, viruses, fungi, and parasites to withstand the effects of medications designed to kill or inhibit their growth. This phenomenon poses a significant threat to global health by rendering standard treatments ineffective, leading to increased morbidity, mortality, and healthcare costs. The misuse and overuse of antibiotics in human medicine, agriculture, and animal husbandry are primary drivers of antibiotic resistance. Factors such as inappropriate prescribing practices, incomplete treatment courses, and the widespread use of antibiotics in livestock contribute to the rapid evolution of resistant strains. Antibiotic resistance not only complicates the treatment of infectious diseases but also jeopardizes advancements in medical procedures such as surgery, chemotherapy, and organ transplantation. Without effective antibiotics, common infections can become life-threatening, and the risk of complications increases substantially. To combat antibiotic resistance effectively, a multifaceted approach is required. This includes promoting responsible antibiotic use, improving surveillance systems to monitor resistance patterns, investing in the development of new antibiotics and alternative therapies, and implementing stringent infection prevention and control measures, see [18, 34, 36, 37, 43].

The authors in [15] suggested and explored a discretized version of a fractional-order multi-drug model for antimicrobial resistance. The study in [15] delved into the effects of adjusting system parameters, unveiling a realm where the system experiences intriguing bifurcations under specific circumstances. Notably, the stability of the model is intricately intertwined with the fractional-order parameter. Within this dynamic framework, a lavish array of behaviors unfolds, including the emergence of Hopf bifurcation, chaotic attractors, and attractor crisis. Elettreby et al. [4] proposed a basic model that examines the competition between drug-resistant and drug-sensitive bacteria, with conditions studied for local stability that align with real-world data. Positive solutions within antimicrobial resistance complex networks are confirmed. The dynamics of identical AMR models are explored across various complex network topologies, revealing the presence of chaotic attractors in all instances. In [13], authors presented a concise mathematical model of multi-drug antimicrobial resistance, capturing the dynamics of susceptible individuals and three distinct classes of infected populations. These classes exhibit varying responses to two antimicrobial drugs, with stability conditions for equilibrium states derived. A multi-objective optimization approach was utilized to determine the minimum drug doses required. A straightforward mathematical fractional-order model to study multi-drug antimicrobial resistance was introduced and examined in [14].

Mathematical models have significantly contributed to enhancing our understanding of various biological phenomena [16]. In the context of epidemics, numerous mathematical models have been developed to explore different aspects, as exemplified by references [22, 23]. Integer-order dynamical systems have been employed to model the optimization of antibiotic usage [28]. Furthermore, Moghadas [29] proposed a model to investigate the impact of imperfect vaccines on disease epidemiology. Overall, the theory of dynamical systems stands as one of the fundamental approaches to developing mathematical models for biological processes [6]. Mondragon et al. [21] developed a mathematical model to analyze the popu-

lation dynamics of bacteria when exposed to multiple antibiotics simultaneously. Their study focused on understanding how the presence of multiple antibiotics affects the evolution of resistance. Ternent et al. [39] examined a mathematical model that considers the resistant mechanisms of bacteria in response to a treatment involving an antibiotic and an anti- virulence drug. They also incorporated the time it takes for drugs to be ingested and excreted from the body into their model, which was formulated using ordinary differential equations. In a study by Dasbasi and Oztürk [9], a model was proposed that takes into account the host's immune system cells and the fundamental mechanisms of bacterial resistance. This model aimed to provide insights into the interplay between the immune response and the development of antibiotic resistance. Dasbasi [8] proposed a model to examine the fractional order bacterial infection model with the effects of anti-virulence drugs and antibiotics. Salman and Ran [35] studied patterns and dynamics in a space-time discrete mathematical model of antibiotic resistance in hospitals with self-diffusion. These studies contribute to our understanding of how different factors, such as multiple antibiotics, anti-virulence drugs, and the immune system, can impact the evolution of antibiotic resistance within the host.

In the case of both antimicrobial resistance and waning vaccination, exposure time plays a significant role, necessitating the inclusion of memory effects. Thus, the application of fractional-order formulations becomes highly relevant in understanding antimicrobial resistance dynamics. An essential aspect to consider is the existence of dynamical analysis and bifurcation in these models, which can provide valuable insights into the complex behavior and stability properties of the systems. This paper presents a fractional-order dynamical system model for studying antimicrobial resistance in the Caputo sense. The model focuses on examining the dynamics of a population facing a bacterial infection, specifically considering different sub-populations, including the susceptible population, the infected and treated population, the infected and untreated population, and the infected population with a resistant strain. The aim is to analyze and understand the dynamics of these sub-populations within the context of antibiotic resistance.

The remaining sections of this article are organized as follows. Section 2 provides preliminary definitions and concepts related to fractional derivative operators. Section 3 presents the mathematical formulation of the proposed fractional-order antibiotic resistance model. It introduces relevant definitions and theorems about the existence, uniqueness, boundedness, and non-negativity of the model's solutions. Moving on to Section 4, the stability analysis of the proposed fractional-order model is conducted. The objective is to assess the stability properties of the system and gain insights into its behavior. In Section 5, the analysis results of the model are presented, and its performance is evaluated through numerical simulations using literature data. Additionally, sensitivity analysis of the reproduction parameters is performed based on these examples. Finally, in Section 6, the paper concludes with a summary of the findings and their implications.

2. Definitions and mathematical preliminaries

In the following section, we will present several essential definitions that will be referenced in subsequent sections, see [11].

Definition 2.1. The Riemann-Liouville fractional integral for a continuous function $\nu : [0, +\infty) \to \mathbb{R}$ can be expressed as follows:

$$ {}_0^{RL}I_t^q \nu(t) = \frac{1}{\Gamma(q)} \int_0^t (t-\tau)^{q-1} \nu(\tau) d\tau, \quad q \in (0,1), \quad t > 0. $$

Definition 2.2. The Riemann-Liouville fractional derivative for a continuous function $\nu : [0, +\infty) \to \mathbb{R}$ is defined by

$$ {}_0^{RL}D_t^{\alpha} \nu(t) = \frac{1}{\Gamma(1-\alpha)} \frac{d}{dt} \int_0^t (t-\tau)^{-\alpha} \nu(\tau) d\tau, \quad \alpha \in (0,1), \quad t > 0. $$

Definition 2.3. The Caputo fractional derivative is a mathematical operator that is used to define the derivative of a continuous function in a fractional order for $\nu : [0, +\infty) \to \mathbb{R}$ can be expressed as follows:

$$ {}_0^C D_t^\alpha \nu(t) = \frac{1}{\Gamma(1-\alpha)} \int_0^t (t-\tau)^{-\alpha} \frac{d}{d\tau} \nu(\tau) d\tau, \quad \alpha \in (0,1), \quad t > 0. $$

3. The model for antibiotic resistance with Caputo fractional derivative

The model as represented using ordinary derivatives appears as follows [3]:

$$ \begin{cases} \frac{dS}{dt}(t) = -b_1\ S(t)[I_1(t) + I_2(t)] - b_2\ S(t)R(t) + b_3\ S(t)[1 - S(t)], \\ \frac{dI_1}{dt}(t) = pb_1\ S(t)[I_1(t) + I_2(t)] - b_4\ I_1(t), \\ \frac{dI_2}{dt}(t) = (1-p)b_1\ S(t)[I_1(t) + I_2(t)] - b_5\ I_2(t), \\ \frac{dR}{dt}(t) = b_2\ S(t)R(t) + b_6\ I_1(t) - b_7\ R(t). \end{cases} \tag{3.1} $$

Table 1 provides a summary of the description of the variables and parameters. All of these parameters are taken to be positive.

Table 1: The state variables and parameters description for the model (3.1).

Variable	Description
S	The proportion of the population that is susceptible
I_1	The proportion of infected and treated population
I_2	The proportion of infected and not treated population
R	The proportion of infected population with resistant strain
b_1^α	The rate at which sensitive strains of the infection spread
b_2^α	The rate at which resistant strains of the infection propagate
b_3^α	The rate of growth for the population of susceptible individuals
b_4^α	Discharge rate for infected and treated individuals
b_5^α	Discharge rate for infected but not treated individuals
b_6^α	The rate of evolution of resistance
b_7^α	Discharge rate for infected individuals with resistant strains
p	The rate of treatment with antibiotics

Fractional-order differential equations extend traditional equations to non-integer orders by incorporating power law memory kernels that establish non-local relationships. These equations serve as a robust tool for characterizing the memory properties and hereditary aspects of intricate phenomena. Rooted in fundamental physical principles, these inquiries pave the way for a new realm of scientific exploration, including innovative theoretical analyses and numerical methods tailored for fractional-order dynamical systems. In contrast to conventional biological models that primarily rely on integer-order dynamics, overlooking the complex memory and hereditary dynamics inherent in biological processes, the incorporation of fractional calculus into the proposed system enables a more sophisticated depiction of the nonlinear and intricate dynamics in operation [3, 11, 14]. This investigation is vital for accurately capturing the nuanced characteristics of the system, as fractional calculus offers a flexible framework better suited to capturing the underlying mechanisms governing biological phenomena. The fractional derivative in the Caputo sense is utilized to replace the integer derivative in the antimicrobial model (3.1), giving rise to the following new model:

$$\begin{cases} {}_0^C D_t^\alpha S(t) = -b_1^\alpha S(t)[I_1(t) + I_2(t)] - b_2^\alpha S(t)R(t) + b_3^\alpha S(t)[1 - S(t)], \\ {}_0^C D_t^\alpha I_1(t) = p^\alpha b_1^\alpha S(t)[I_1(t) + I_2(t)] - b_4^\alpha I_1(t), \\ {}_0^C D_t^\alpha I_2(t) = (1 - p^\alpha) b_1^\alpha S(t)[I_1(t) + I_2(t)] - b_5^\alpha I_2(t), \\ {}_0^C D_t^\alpha R(t) = b_2^\alpha S(t)R(t) + b_6^\alpha I_1(t) - b_7^\alpha R(t), \end{cases} \tag{3.2}$$

given the positive initial conditions as $S(0) = S_0$, $I_1(0) = I_{1,0}$, $I_2(0) = I_{2,0}$, $R(0) = R_0$. Integer derivatives are used to produce equation (3.1), and the model (3.2) is formulated by employing Caputo fractional derivatives. Memory is connected in particular to fractional order derivatives. To describe the crossover behaviors and memory effects of the systems, fractional derivatives are used. We can project the data with more variations if we swap the integer-order model out for the fractional-order model (in the Caputo sense). We can choose the most suitable value that follows the projection of the real data and provides us with the best fix for a later period by changing the fractional order α values. Typically, the Caputo variant is selected for depicting biological models due to its clear physical interpretation of the provided data. In most cases where a fractional derivative concept is necessary, the Caputo fractional derivative adequately addresses the requirements.

3.1. Some properties of the solutions of the model (3.2)

To establish the boundedness and nonnegativity of the solution of model (3.2) for all time $t \geqslant t_0$, we employ the generalized mean value theorem [31] in the following manner. This result holds true when considering positive initial conditions and parameters.

Lemma 3.1. *Suppose* $\nu(t)$ *and* ${}_0^C D_t^\alpha \nu(t)$ *belong to* $C[0, t_f]$. *Hence, we get*

$$\nu(t) = \nu(0) + \frac{1}{\Gamma(\alpha)} {}_0^C D_\xi^\alpha \nu(\xi).(t - t_0)^\alpha, \quad 0 \leqslant \xi \leqslant t, \ \forall t \in (0, t_f].$$

Corollary 3.2. *Suppose* $\nu(t)$, ${}_0^C D_t^\alpha \nu(t)$ *belong to* $C[0, t_f]$, *and* $\alpha \in (0, 1]$. *From Lemma 3.1 if*

(i) ${}_0^C D_t^\alpha \nu(t) \geqslant 0$, $\forall t \in (0, t_f)$, *then* $\nu(t)$ *is non-decreasing*, $\forall t \in [0, t_f]$.
(ii) ${}_0^C D_t^\alpha \nu(t) \leqslant 0$, $\forall t \in (0, t_f)$, *then* $\nu(t)$ *is non-increasing*, $\forall t \in [0, t_f]$.

We can now present the following findings.

Theorem 3.3. *For the model (3.2), the region* $\Omega_+ = \{(S, I_1, I_2, R); S > 0, I_1 \geqslant 0, I_2 \geqslant 0, R \geqslant 0\}$ *is a positive invariant.*

Proof. Existence and uniqueness of the solution for model (3.2) on the time interval (0,∞) have been established in previous studies [5, 27]. Based on the model (3.2), we obtain the following expression:

$$\begin{cases} {}_0^C D_t^\alpha S\big|_{S=0} = 0, \\ {}_0^C D_t^\alpha I_1\big|_{I_1=0} = p^\alpha b_1^\alpha S(t) I_2(t) \geqslant 0, \\ {}_0^C D_t^\alpha I_2\big|_{I_2=0} = (1 - p^\alpha) b_1^\alpha S(t) I_1(t) \geqslant 0, \\ {}_0^C D_t^\alpha R\big|_{R=0} = b_6^\alpha I_1(t) \geqslant 0. \end{cases} \tag{3.3}$$

From Corollary 3.2 and (3.3) and from our analysis, we can confidently conclude that the region Ω_+ acts as a positive invariant. As a result, the solution will consistently stay within Ω_+, thereby guaranteeing its nonnegativity throughout the entire process. □

In what follows, for our fractional model (3.2), we investigate the existence and uniqueness of solutions, see [1]. In order to ensure the existence and uniqueness of solutions for the fractional-order system (3.2) within the region $\Xi \times (0, T]$, we aim to identify a sufficient condition,

$$\Xi = \left\{(S, I_1, I_2, R) \in \mathbb{R}^4 : \max(|S|, |I_1|, |I_2|, |R|) \leqslant \mu\right\}.$$

Consider a mapping defined in the following form: $\psi = (\psi_1, \psi_2, \psi_3, \psi_4)$, where the elements on the right-hand side are defined as

$$\begin{cases} \psi_1(t, S(t)) = -b_1^\alpha S(t)[I_1(t) + I_2(t)] - b_2^\alpha S(t)R(t) + b_3^\alpha S(t)[1 - S(t)], \\ \psi_2(t, I_1(t)) = p^\alpha b_1^\alpha S(t)[I_1(t) + I_2(t)] - b_4^\alpha I_1(t), \\ \psi_3(t, I_2(t)) = (1 - p^\alpha) b_1^\alpha S(t)[I_1(t) + I_2(t)] - b_5^\alpha I_2(t), \\ \psi_4(t, R(t)) = b_2^\alpha S(t)R(t) + b_6^\alpha I_1(t) - b_7^\alpha R(t). \end{cases} \tag{3.4}$$

The Volterra type system below, where $\alpha \in (0, 1)$ is a fractional integral in the Caputo sense, is the result of a straightforward application of Caputo sense fractional integral operators.

$$\begin{cases} S(t) - S(0) = \frac{1}{\Gamma(\alpha)} \int_0^t (t - \tau)^{\alpha-1} \psi_1(\tau, S) d\tau, \\ I_1(t) - I_1(0) = \frac{1}{\Gamma(\alpha)} \int_0^t (t - \tau)^{\alpha-1} \psi_2(\tau, I_1)\, d\tau, \\ I_2(t) - I_2(0) = \frac{1}{\Gamma(\alpha)} \int_0^t (t - \tau)^{\alpha-1} \psi_3(\tau, I_2)\, d\tau, \\ R(t) - R(0) = \frac{1}{\Gamma(\alpha)} \int_0^t (t - \tau)^{\alpha-1} \psi_4(\tau, R) d\tau. \end{cases} \tag{3.5}$$

In what follows, we prove that $\psi_i,\ i = 1, 2, 3, 4$ verify the Lipschitz condition. Also, we prove under some conditions that $\psi_i,\ i = 1, 2, 3, 4$ can be contractions. We prove only the case of ψ_1, in a similar technique, the other cases $\psi_i,\ i = 2, 3, 4$ can be proved.

Theorem 3.4. *If* $2\mu b_1^\alpha + \mu b_2^\alpha + b_3^\alpha + 2\mu b_3^\alpha < 1$, *then* ψ_1 *satisfies both Lipschitz and contraction conditions.*

Proof. From (3.4), we get

$$\begin{aligned} \|\psi_1(t, S) - \psi_1(t, S_1)\| &= \|-b_1^\alpha [I_1(t) + I_2(t)] - b_2^\alpha R(t) + b_3^\alpha [1 - (S(t) + S(t_1))]\| \, \|S(t) - S(t_1)\| \\ &\leqslant (2\mu b_1^\alpha + \mu b_2^\alpha + b_3^\alpha + 2\mu b_3^\alpha) \, \|S(t) - S(t_1)\| . \end{aligned}$$

Now setting $W_1 = 2\mu b_1^\alpha + \mu b_2^\alpha + b_3^\alpha + 2\mu b_3^\alpha$, we obtain

$$\|\psi_1(t, S) - \psi_1(t, S_1)\| \leqslant W_1 \|S(t) - S(t_1)\| . \tag{3.6}$$

Hence, the Lipschitz condition is verified for ψ_1. If $0 < W_1 = 2\mu b_1^\alpha + \mu b_2^\alpha + b_3^\alpha + 2\mu b_3^\alpha < 1$, then the contraction follows. Similarly, we can obtain the Lipschitz condition for the remaining Kernels:

$$\begin{cases} \|\psi_2(t, I_1(t)) - \psi_2(t, I_1(t_1))\| \leqslant W_2 \|I_1(t) - I_1(t_1)\| , \\ \|\psi_3(t, I_2(t)) - \psi_3(t, I_2(t_1))\| \leqslant W_3 \|I_2(t) - I_2(t_1)\| , \\ \|\psi_4(t, R(t)) - \psi_4(t, R(t_1))\| \leqslant W_4 \|R(t) - R(t_1)\| . \end{cases}$$

□

Recursively, we rewrite (3.5) as follows

$$\begin{cases} S_n(t) - S(0) = \frac{1}{\Gamma(\alpha)} \int_0^t (t - \tau)^{\alpha-1} \psi_1(\tau, S_{n-1})\, d\tau, \\ I_{1,\,n}(t) - I_1(0) = \frac{1}{\Gamma(\alpha)} \int_0^t (t - \tau)^{\alpha-1} \psi_2(\tau, I_{1,n-1})\, d\tau, \\ I_{2,n}(t) - I_2(0) = \frac{1}{\Gamma(\alpha)} \int_0^t (t - \tau)^{\alpha-1} \psi_3(\tau, I_{2,n-1})\, d\tau, \\ R_n(t) - R(0) = \frac{1}{\Gamma(\alpha)} \int_0^t (t - \tau)^{\alpha-1} \psi_4(\tau, R_{n-1})\, d\tau. \end{cases} \tag{3.7}$$

By utilizing the recursive form of successive differences between terms in system (3.7), we can derive the following expression:

$$\begin{cases} \varphi_{1n}(t) = S_n(t) - S_{n-1}(t) = \frac{1}{\Gamma(\alpha)} \int_0^t (t - \tau)^{\alpha-1} (\psi_1(\tau, S_{n-1}) - \psi_1(\tau, S_{n-2})) d\tau, \\ \varphi_{2n}(t) = I_{1,\,n}(t) - I_{1,\,n-1}(t) = \frac{1}{\Gamma(\alpha)} \int_0^t (t - \tau)^{\alpha-1} (\psi_2(\tau, I_{1,n-1}) - \psi_2(\tau, I_{1,n-2})) d\tau, \\ \varphi_{3n}(t) = I_{2,n}(t) - I_{2,\,n-1}(t) = \frac{1}{\Gamma(\alpha)} \int_0^t (t - \tau)^{\alpha-1} (\psi_3(\tau, I_{2,n-1}) - \psi_3(\tau, I_{2,n-2})) d\tau, \\ \varphi_{4n}(t) = R_n(t) - R_{n-1}(t) = \frac{1}{\Gamma(\alpha)} \int_0^t (t - \tau)^{\alpha-1} (\psi_4(\tau, R_{n-1}) - (\psi_4(\tau, R_{n-2})) d\tau. \end{cases}$$

With the initial conditions $S(0) = S_0, I_1(0) = I_{1,0}, I_2(0) = I_{2,0}, R(0) = R_0$. Hence,

$$\begin{aligned}\|\varphi_{1n}(t)\| = \|S_n(t) - S_{n-1}(t)\| &= \left\| \frac{1}{\Gamma(\alpha)} \int_0^t (t-\tau)^{\alpha-1} (\psi_1(\tau, S_{n-1}) - \psi_1(\tau, S_{n-2}))\, d\tau \right\| \\ &\leqslant \frac{1}{\Gamma(\alpha)} \left\| \frac{1}{\Gamma(\alpha)} \int_0^t (t-\tau)^{\alpha-1} (\psi_1(\tau, S_{n-1}) - \psi_1(\tau, S_{n-2}))\, d\tau \right\|.\end{aligned}$$

Using Lipschitz condition in (3.6) gives

$$\|\varphi_{1n}(t)\| \leqslant \frac{1}{\Gamma(\alpha)} W_1 \int_0^t (t-\tau)^{\alpha-1} \|S_{n-1} - S_{n-2}\|\, d\tau.$$

Thus, we have

$$\|\varphi_{1n}(t)\| \leqslant \frac{1}{\Gamma(\alpha)} W_1 \int_0^t (t-\tau)^{\alpha-1} \left\|\varphi_{1(n-1)}(\tau)\right\| d\tau. \tag{3.8}$$

Similarly, we can obtain

$$\begin{cases} \|\varphi_{2n}(t)\| \leqslant \frac{1}{\Gamma(\alpha)} W_2 \int_0^t (t-\tau)^{\alpha-1} \left\|\varphi_{2(n-1)}(\tau)\right\| d\tau, \\ \|\varphi_{3n}(t)\| \leqslant \frac{1}{\Gamma(\alpha)} W_3 \int_0^t (t-\tau)^{\alpha-1} \left\|\varphi_{3(n-1)}(\tau)\right\| d\tau, \\ \|\varphi_{4n}(t)\| \leqslant \frac{1}{\Gamma(\alpha)} W_4 \int_0^t (t-\tau)^{\alpha-1} \left\|\varphi_{4(n-1)}(\tau)\right\| d\tau. \end{cases}$$

Consequently, each n^{th} term of each state variable of (3.4) can be expressed as

$$\begin{cases} S_n(t) = \sum_{j=0}^n \varphi_{1j}(t), \\ I_{1,\,n}(t) = \sum_{j=0}^n \varphi_{2j}(t), \\ I_{2,n}(t) = \sum_{j=0}^n \varphi_{3j}(t), \\ R_n(t) = \sum_{j=0}^n \varphi_{4j}(t). \end{cases}$$

The ensuing theorem provides a proof of the uniqueness of the solution to the fractional model (3.2) in the Caputo sense.

Theorem 3.5. *Assume that*

$$\frac{1}{\Gamma(\alpha)} b^{\epsilon} W_i < 1, \text{ for } i = 1, 2, 3, 4.$$

Then the fractional model (3.2) *has solution for* $t \in [0, T]$.

Proof. The following equalities are true when taking into account the criteria stated in (3.6), the inequalities (3.8) and (3.7), and the recursive method:

$$\begin{cases} \|\varphi_{1n}(t)\| \leqslant \|S_0(t)\| \left[\frac{W_1}{\Gamma(\alpha)} b^{\epsilon}\right]^n, \\ \|\varphi_{2n}(t)\| \leqslant \|I_{1,0}(t)\| \left[\frac{W_2}{\Gamma(\alpha)} b^{\epsilon}\right]^n, \\ \|\varphi_{3n}(t)\| \leqslant \|I_{2,0}(t)\| \left[\frac{W_3}{\Gamma(\alpha)} b^{\epsilon}\right]^n, \\ \|\varphi_{4n}(t)\| \leqslant \|R_0(t)\| \left[\frac{W_4}{\Gamma(\alpha)} b^{\epsilon}\right]^n. \end{cases} \tag{3.9}$$

It follows that each of the aforementioned sequences listed above exists and satisfies:

$$\lim_{n\to\infty} \|\varphi_{in}(t)\| \to 0, i = 1, 2, 3, 4.$$

When the triangle inequality is applied, the inequalities of (3.9) become

$$\begin{cases} \|S_{n+k}(t)-S_n(t)\| \leqslant \sum_{j=n+1}^{n+k} \mathcal{K}_1^j = \frac{\mathcal{K}_1^{n+1}-\mathcal{K}_1^{n+k+1}}{1-\mathcal{K}_1}, \\ \|I_{1,n+k}(t)-I_{1,n}(t)\| \leqslant \sum_{j=n+1}^{n+k} \mathcal{K}_2^j = \frac{\mathcal{K}_2^{n+1}-\mathcal{K}_2^{n+k+1}}{1-\mathcal{K}_2}, \\ \|I_{2,n+k}(t)-I_{2,n}(t)\| \leqslant \sum_{j=n+1}^{n+k} \mathcal{K}_3^j = \frac{\mathcal{K}_3^{n+1}-\mathcal{K}_3^{n+k+1}}{1-\mathcal{K}_3}, \\ \|R_{n+k}(t)-R_n(t)\| \leqslant \sum_{j=n+1}^{n+k} \mathcal{K}_4^j = \frac{\mathcal{K}_4^{n+1}-\mathcal{K}_4^{n+k+1}}{1-\mathcal{K}_4}, \end{cases}$$

where $\frac{W_i}{\Gamma(\alpha)}b^\epsilon < 1$, $\mathcal{K}_i = \left[\frac{W_i}{\Gamma(\alpha)}b^\epsilon\right]^n$, i=1,2,3,4. Hence, S_n, $I_{1,n}$, $I_{2,n}$, and R_n are considered as uniformly convergent Cauchy sequences (see [26, 32]). If we take the limit of (3.7) with $n \to \infty$, we come to the conclusion that the limits of the aforementioned sequences are equal to the solutions of model (3.2). This completes the proof. □

4. Analysis of equilibrium points and their stability

Assume that the fractional order model is given as follows

$$ {}_0^C D_t^\alpha \mathbf{x} = \mathbf{f}(\mathbf{x}), \alpha \in (0,\ 1), x_i(0) = k_i,\ i = 1,2,\ldots,n,$$

where k_i are initial conditions, $\mathbf{f} = [f_1, f_2, \ldots, f_n]^T$: $\mathbb{R}^n \to \mathbb{R}^n$ and $\mathbf{x}(t) = [x_1(t), x_2(t), \ldots, x_n(t)]^T \in \mathbb{R}^n$. The steady states or equilibrium points (EPs) of the above system can be obtained by taking ${}_0^C D_t^\alpha \mathbf{x} = 0$. Hence, by solving nonlinear algebraic equations $\mathbf{f}(\mathbf{x}^*) = \mathbf{0}$, the EPs can be obtained [32]. Let $\mathbf{J}(\mathbf{x}^*)$ be the Jacobian matrix $\mathbf{J} = \left(\frac{\partial \mathbf{f}}{\partial \mathbf{x}}\right)\Big|_{EPs} = \left(\frac{\partial(f_1, f_2, \ldots, f_n)}{\partial(x_1, x_2, \ldots, x_n)}\right)\Big|_{EPs}$ of above system at equilibrium point $\mathbf{x} = \mathbf{x}^*$. The eigen values of $\mathbf{J}(\mathbf{x}^*)$ are λ_i, where $i = 1, 2, \ldots, n$. Then

- equilibrium point $\mathbf{x}^*$ is locally asymptotically stable if and only if $\left|\arg(\lambda_i)\right| > \frac{\alpha\pi}{2}$ (Matignon conditions);
- equilibrium point $\mathbf{x}^*$ is stable if and only if $\left|\arg(\lambda_i)\right| \geqslant \frac{\alpha\pi}{2}$, and eigenvalues with $\left|\arg(\lambda_i)\right| = \frac{\alpha\pi}{2}$ have the same geometric multiplicity and algebraic multiplicity; and
- equilibrium point $\mathbf{x}^*$ is unstable if and only if there exists eigenvalue λ_i of the Jacobian matrix $\mathbf{J}(\mathbf{x}^*)$ such that $\left|\arg(\lambda_i)\right| < \frac{\alpha\pi}{2}$.
- The stable and unstable regions for fractional order system are shown in Figure 1.

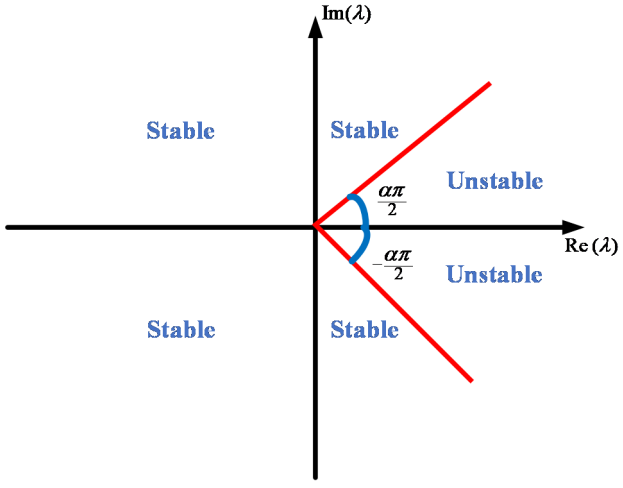

Figure 1: Stability region of the fractional-order system (3.2).

By setting the right-hand side of model (3.2) equal to zero and solving the resulting system, we can determine the solutions,

$$\begin{cases} -b_1^\alpha S(t)[I_1(t)+I_2(t)]-b_2^\alpha S(t)R(t)+b_3^\alpha S(t)[1-S(t)]=0, \\ p^\alpha b_1^\alpha S(t)[I_1(t)+I_2(t)]-b_4^\alpha I_1(t)=0, \\ (1-p^\alpha)b_1^\alpha S(t)[I_1(t)+I_2(t)]-b_5^\alpha I_2(t)=0, \\ b_2^\alpha S(t)R(t)+b_6^\alpha I_1(t)-b_7^\alpha R(t)=0, \end{cases}$$

we can find the values of S, I_1, I_2, and R, $E_i=\left(S^{(i)},I_1^{(i)},I_2^{(i)},R^{(i)}\right), i\in\{1,2,3,4\}$,

$$\begin{cases} S^{(1)}=0, \\ I_1^{(1)}=0, \\ I_2^{(1)}=0, \\ R^{(1)}=0, \end{cases} \quad \begin{cases} S^{(2)}=1, \\ I_1^{(2)}=0, \\ I_2^{(2)}=0, \\ R^{(2)}=0, \end{cases} \quad \begin{cases} S^{(3)}=\frac{b_7^\alpha}{b_2^\alpha}, \\ I_1^{(3)}=0, \\ I_2^{(3)}=0, \\ R^{(3)}=\frac{b_3^\alpha\left(b_2^\alpha-b_7^\alpha\right)}{b_2^{2\alpha}}, \end{cases}$$

$$\begin{cases} S^{(4)}=\frac{b_4^\alpha b_5^\alpha}{b_1^\alpha(p^\alpha b_5^\alpha-\left((-1+p^\alpha)b_4^\alpha\right))}, \\ I_1^{(4)}=\frac{p^\alpha b_3^\alpha b_5^\alpha(-b_4^\alpha b_5^\alpha+b_1^\alpha(-((-1+p^\alpha)b_4^\alpha)+p^\alpha b_5^\alpha))(-b_2^\alpha b_4^\alpha b_5^\alpha+b_1^\alpha(-((-1+p^\alpha)b_4^\alpha)+p^\alpha b_5^\alpha)b_7^\alpha)}{b_1^{2\alpha}((-1+p^\alpha)b_4^\alpha-p^\alpha b_5^\alpha)^2(b_2^\alpha b_5^\alpha(-b_4^\alpha+p^\alpha b_6^\alpha)+b_1^\alpha(-((-1+p^\alpha)b_4^\alpha)+p^\alpha b_5^\alpha)b_7^\alpha)}, \\ I_2^{(4)}=\frac{(-1+p^\alpha)b_3^\alpha b_4^\alpha((-1+p^\alpha)b_1^\alpha b_4^\alpha+(-p^\alpha b_1^\alpha+b_4^\alpha)b_5^\alpha)(b_2^\alpha b_4^\alpha b_5^\alpha+b_1^\alpha((-1+p^\alpha)b_4^\alpha-p^\alpha b_5^\alpha)b_7^\alpha)}{b_1^{2\alpha}((-1+p^\alpha)b_4^\alpha-p^\alpha b_5^\alpha)^2(b_2^\alpha b_5^\alpha(b_4^\alpha-p^\alpha b_6^\alpha)+b_1^\alpha((-1+p^\alpha)b_4^\alpha-p^\alpha b_5^\alpha)b_7^\alpha)}, \\ R^{(4)}=\frac{p^\alpha b_3^\alpha b_5^\alpha(-b_4^\alpha b_5^\alpha+b_1^\alpha(-((-1+p^\alpha)b_4^\alpha)+p^\alpha b_5^\alpha))b_6^\alpha}{b_1^\alpha((-1+p^\alpha)b_4^\alpha-p^\alpha b_5^\alpha)(b_2^\alpha b_5^\alpha(b_4^\alpha-p^\alpha b_6^\alpha)+b_1^\alpha((-1+p^\alpha)b_4^\alpha-p^\alpha b_5^\alpha)b_7^\alpha)}. \end{cases}$$

Therefore, there are four EPs for the model (3.2). Now, we investigate the system's local stability of the equilibria of model (3.2). By examining the Jacobian matrix of system (3.2) at these equilibria, it is found that:

$$J=\begin{pmatrix} -((I_1+I_2)b_1^\alpha)-Rb_2^\alpha+(1-2S)b_3^\alpha & -Sb_1^\alpha & -Sb_1^\alpha & -Sb_2^\alpha \\ p^\alpha(I_1+I_2)b_1^\alpha & p^\alpha Sb_1^\alpha-b_4^\alpha & p^\alpha Sb_1^\alpha & 0 \\ -((-1+p^\alpha)(I_1+I_2)b_1^\alpha) & -((-1+p^\alpha)Sb_1^\alpha) & -((-1+p^\alpha)Sb_1^\alpha)-b_5^\alpha & 0 \\ Rb_2^\alpha & b_6^\alpha & 0 & Sb_2^\alpha-b_7^\alpha \end{pmatrix}.$$

It is simple to verify that the Jacobian matrix calculated at the trivial equilibrium state

$$E_1=\left(S^{(1)},I_1^{(1)},I_2^{(1)},R^{(1)}\right)$$

equals

$$J_1=\begin{pmatrix} b_3^\alpha & 0 & 0 & 0 \\ 0 & -b_4^\alpha & 0 & 0 \\ 0 & 0 & -b_5^\alpha & 0 \\ 0 & b_6^\alpha & 0 & -b_7^\alpha \end{pmatrix}.$$

It has the following eigenvalues:

$$\begin{cases} \lambda_1^{(1)}=b_3^\alpha>0, \\ \lambda_2^{(1)}=-b_4^\alpha<0, \\ \lambda_3^{(1)}=-b_5^\alpha<0, \\ \lambda_3^{(1)}=-b_7^\alpha<0. \end{cases}$$

Then, the equilibrium point E_1 is unstable since one of these eigenvalues is positive. Hence, we have the following proposition.

Proposition 4.1. *The equilibrium point* E_1 *is unstable equilibrium point for model* (3.2).

Proposition 4.2. $\left|\tan^{-1}\frac{\nu_1}{u_1}\right| > \frac{\alpha\pi}{2}$, $u_1 = \frac{1}{2}\left(b_1^\alpha - b_4^\alpha - b_5^\alpha\right)$,

$$\nu_1 = \frac{1}{2}\sqrt{-(-b_1^\alpha + b_4^\alpha + b_5^\alpha)^2 + 4(b_4^\alpha b_5^\alpha + b_1^\alpha((-1+p^\alpha)b_4^\alpha - p^\alpha b_5^\alpha))},$$

and $b_2^\alpha - b_7^\alpha < 0$, *when the second equilibrium point* E_2 *exists, it is locally asymptotically stable.*

Proof. The Jacobian matrix evaluated at the equilibrium point E_2 can be expressed as follows:

$$J_2 = \begin{pmatrix} -b_3^\alpha & -b_1^\alpha & -b_1^\alpha & -b_2^\alpha \\ 0 & p^\alpha b_1^\alpha - b_4^\alpha & p^\alpha b_1^\alpha & 0 \\ 0 & -((-1+p^\alpha)b_1^\alpha) & -((-1+p^\alpha)b_1^\alpha) - b_5^\alpha & 0 \\ 0 & b_6^\alpha & 0 & b_2^\alpha - b_7^\alpha \end{pmatrix}.$$

It has the following eigenvalues

$$\begin{cases} \lambda_1^{(2)} = -b_3^\alpha, \\ \lambda_{2,3}^{(2)} = u_1 \pm i\nu_1;\ u_1 = \frac{1}{2}\left(b_1^\alpha - b_4^\alpha - b_5^\alpha\right), \nu_1 = \frac{1}{2}\sqrt{-(-b_1^\alpha + b_4^\alpha + b_5^\alpha)^2 + 4(b_4^\alpha b_5^\alpha + b_1^\alpha((-1+p^\alpha)b_4^\alpha - p^\alpha b_5^\alpha))}, \\ \lambda_4^{(2)} = b_2^\alpha - b_7^\alpha, \end{cases}$$

Then, the equilibrium point E_2 is locally asymptotically stable if $\left|\tan^{-1}\frac{\nu_1}{u_1}\right| > \frac{\alpha\pi}{2}$, and $\lambda_4^{(2)} < 0$. □

Proposition 4.3. *If* $\left|\tan^{-1}\frac{\nu_2}{u_2}\right| > \frac{\alpha\pi}{2}$; $u_2 = -\frac{1}{2b_2^\alpha}\left(b_3^\alpha b_7^\alpha\right), \nu_2 = -\frac{1}{2b_2^\alpha}\left(\sqrt{4b_2^{2\alpha}b_3^\alpha b_7^\alpha - \left(4b_2^\alpha b_3^\alpha + b_3^{2\alpha}\right)b_7^{2\alpha}}\right)$, $\left|\tan^{-1}\frac{\nu_3}{u_3}\right| > \frac{\alpha\pi}{2}$; $u_3 = \frac{1}{2b_2^\alpha}\left(b_2^\alpha\left(-b_4^\alpha - b_5^\alpha\right) + b_1^\alpha b_7^\alpha\right)$,

$$\nu_3 = -\frac{1}{2b_2^\alpha}\sqrt{-\left(b_2^\alpha\left(b_4^\alpha + b_5^\alpha\right) - b_1^\alpha b_7^\alpha\right)^2 + 4\left(b_2^{2\alpha}b_4^\alpha b_5^\alpha + b_1^\alpha b_2^\alpha\left(\left(-1+p^\alpha\right)b_4^\alpha - p^\alpha b_5^\alpha\right)b_7^\alpha\right)},$$

and $b_2^\alpha - b_7^\alpha < 0$, *if the third equilibrium point, denoted as* E_3 *exists, it is locally asymptotically stable.*

Proof. The Jacobian matrix evaluated at the equilibrium point E_3 can be expressed as follows:

$$J_3 = \begin{pmatrix} -b_2^{-\alpha}b_3^\alpha b_7^\alpha & -b_1^\alpha b_2^{-\alpha}b_7^\alpha & -b_1^\alpha b_2^{-\alpha}b_7^\alpha & -b_7^\alpha \\ 0 & -b_4^\alpha + p^\alpha b_1^\alpha b_2^{-\alpha}b_7^\alpha & p^\alpha b_1^\alpha b_2^{-\alpha}b_7^\alpha & 0 \\ 0 & -((-1+p^\alpha)b_1^\alpha b_2^{-\alpha}b_7^\alpha) & -b_5^\alpha - (-1+p^\alpha)b_1^\alpha b_2^{-\alpha}b_7^\alpha & 0 \\ b_3^\alpha(1 - b_2^{-\alpha}b_7^\alpha) & b_6^\alpha & 0 & 0 \end{pmatrix}.$$

It has the following eigenvalues

$$\begin{cases} \lambda_{1,2}^{(3)} = u_2 \pm i\nu_2;\ u_2 = -\frac{1}{2b_2^\alpha}\left(b_3^\alpha b_7^\alpha\right), \nu_2 = -\frac{1}{2b_2^\alpha}\left(\sqrt{4b_2^{2\alpha}b_3^\alpha b_7^\alpha - \left(4b_2^\alpha b_3^\alpha + b_3^{2\alpha}\right)b_7^{2\alpha}}\right), \\ \lambda_{3,4}^{(3)} = u_3 \pm i\nu_3;\ u_3 = \frac{1}{2b_2^\alpha}\left(b_2^\alpha\left(-b_4^\alpha - b_5^\alpha\right) + b_1^\alpha b_7^\alpha\right), \\ \nu_3 = -\frac{1}{2b_2^\alpha}\sqrt{-\left(b_2^\alpha\left(b_4^\alpha + b_5^\alpha\right) - b_1^\alpha b_7^\alpha\right)^2 + 4\left(b_2^{2\alpha}b_4^\alpha b_5^\alpha + b_1^\alpha b_2^\alpha\left(\left(-1+p^\alpha\right)b_4^\alpha - p^\alpha b_5^\alpha\right)b_7^\alpha\right)}. \end{cases}$$

Then, the equilibrium point E_3 is locally asymptotically stable if $\left|\tan^{-1}\frac{\nu_2}{u_2}\right| > \frac{\alpha\pi}{2}$ and $\left|\tan^{-1}\frac{\nu_3}{u_3}\right| > \frac{\alpha\pi}{2}$. □

Now, we will find the basic reproduction number $\mathcal{R}_0$ based on the next generation matrix technique [10, 24, 38, 40]. Hence, $\mathcal{R}_0$ can be calculated by $\mathcal{R}_0 = \rho\left(\mathcal{F}\mathcal{V}^{-1}\right)$. Here, ρ represents the spectral radius of the matrix $\mathcal{F}\mathcal{V}^{-1}$, with $\mathcal{F}, \mathcal{V}$ defined as follows. Define the next two matrices:

$$\mathcal{F} = \begin{bmatrix} p^\alpha b_1^\alpha & p^\alpha b_1^\alpha & 0 \\ (1-p^\alpha)b_1^\alpha & (1-p^\alpha)b_1^\alpha & 0 \\ b_6^\alpha & 0 & b_2^\alpha \end{bmatrix} \quad \text{and} \quad \mathcal{V} = \begin{bmatrix} b_4^\alpha & 0 & 0 \\ 0 & b_5^\alpha & 0 \\ 0 & 0 & b_7^\alpha \end{bmatrix}.$$

Then

$$\mathcal{FV}^{-1} = \begin{bmatrix} \frac{p^\alpha b_1^\alpha}{b_4^\alpha} & \frac{p^\alpha b_1^\alpha}{b_5^\alpha} & 0 \\ \frac{(1-p^\alpha) b_1^\alpha}{b_4^\alpha} & \frac{(1-p^\alpha) b_1^\alpha}{b_5^\alpha} & 0 \\ \frac{b_6^\alpha}{b_4^\alpha} & 0 & \frac{b_2^\alpha}{b_7^\alpha} \end{bmatrix}.$$

Thus, we have

$$\mathcal{R}_0 = \max\left\{0, \frac{b_2^\alpha}{b_7^\alpha}, \frac{b_1^\alpha(b_4^\alpha - p^\alpha b_4^\alpha + p^\alpha b_5^\alpha)}{b_4^\alpha b_5^\alpha}\right\}.$$

If $\mathcal{R}_0 < 1$, it follows that the disease-free equilibrium point E_2 is globally stable. The local stability for the fourth equilibrium point $E_4 = \left(S^{(4)}, I_1^{(4)}, I_2^{(4)}, R^{(4)}\right)$ can be investigated numerically due to its complexity. Figures 2 and 3 depict the stability regions of the equilibrium point E_4 in the parameter space of model (3.2). From Figure 2, it is observed that stability region in $b_1 - b_2$ space shrinks when the value of discharge rate for infected individuals with resistant strains is increased. The equilibrium point E_4 losses its stability for small values of b_1 and relatively moderate to large values of b_2, see Figure 3. The value of b_7 also affects the stability of E_4 as illustrated in Figure 3.

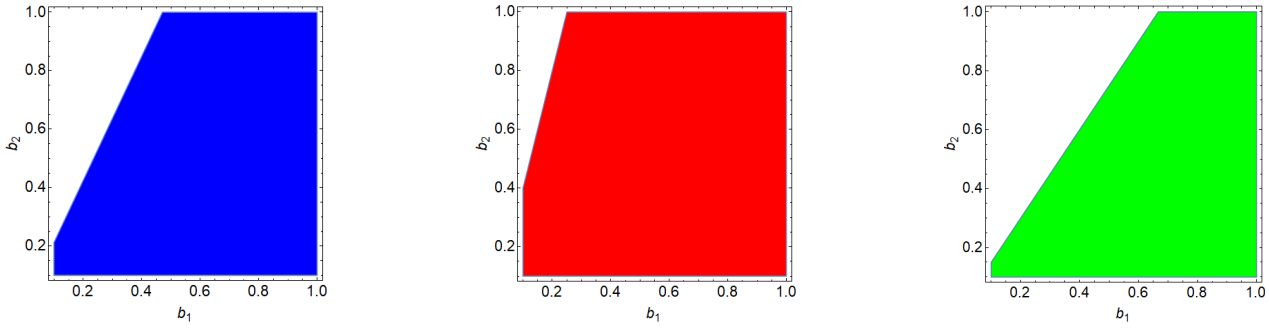

(a) **(b)** **(c)**

Figure 2: The stability regions for E_4 in $b_1 - b_2$ space of parameters of model (3.2) for the following case: (a) $b_7 = 0.06$; (b) $b_7 = 0.03$; and (c) $b_7 = 0.08$. The other values of parameters are $p = 0.1$, $b_3 = 0.4$, $b_4 = 0.02$, $b_5 = 0.03$, $b_6 = 0.5$, and $\alpha = 0.9$.

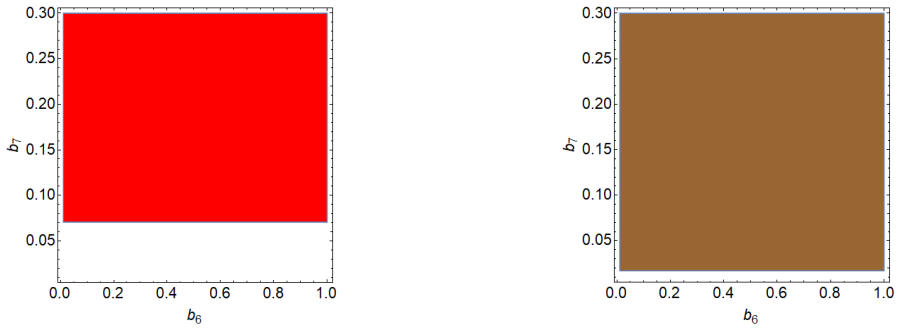

(a) **(b)**

Figure 3: The stability regions for E_4 in $b_6 - b_7$ space of parameters of model (3.2) for the following case: (a) $b_1 = 0.2$, $b_2 = 0.5$, and (b) $b_1 = 0.5$, $b_2 = 0.3$, while the other values of parameters are $p = 0.1$, $b_3 = 0.4$, $b_4 = 0.02$, $b_5 = 0.03$, and $\alpha = 0.9$.

5. Simulation and discussion

In this section, we aim to utilize an efficient numerical technique to obtain the numerical solutions of model (3.2). The method employed is an enhanced version of the well-known Adams-Bashforth-Moulton (ABM) integrator, commonly used for numerical simulations of first-order differential equations [7, 12, 19, 30, 33, 41]. We employ a predictor-corrector scheme based on the Adams-Bashforth-Moulton algorithm. The stability analysis of this numerical scheme can be found in [1]. To numerically simulate

fractional Initial Value Problems (IVPs) with Caputo derivatives, a foundational understanding of the numerical method is essential. The fractional Adams-Bashforth-Moulton technique is comprehensively outlined in the subsequent formulas.

Let the domain of the solution be $[0, T]$ and, $n = 0, 1, 2, \ldots, N$, where $h = T/N$, $t_n = nh$ and let

$$\begin{cases} {}_0^C D_t^\alpha S(t) = \psi_1(t, S(t)), \\ {}_0^C D_t^\alpha I_1(t) = \psi_2(t, I_1(t)), \\ {}_0^C D_t^\alpha I_2(t) = \psi_3(t, I_2(t)), \\ {}_0^C D_t^\alpha R(t) = \psi_4(t, R(t)). \end{cases}$$

Then

$$\begin{cases} S(t_{n+1}) = \sum_{i=0}^{\lceil\alpha\rceil-1} S_0^{(i)} \frac{t_{n+1}^{i+1}}{i!} + \frac{h^\alpha}{\Gamma(\alpha+2)} \psi_1(t_{n+1}, S^p(t_{n+1})) + \frac{h^\alpha}{\Gamma(\alpha+2)} \sum_{j=0}^{n} \lambda_{j,n+1} \psi_1(t_j, S(t_j)), \\ I_1(t_{n+1}) = \sum_{i=0}^{\lceil\alpha\rceil-1} I_{1,0}^{(i)} \frac{t_{n+1}^{i+1}}{i!} + \frac{h^\alpha}{\Gamma(\alpha+2)} \psi_2(t_{n+1}, I_1^p(t_{n+1})) + \frac{h^\alpha}{\Gamma(\alpha+2)} \sum_{j=0}^{n} \lambda_{j,n+1} \psi_2(t_j, I_1(t_j)), \\ I_2(t_{n+1}) = \sum_{i=0}^{\lceil\alpha\rceil-1} I_{2,0}^{(i)} \frac{t_{n+1}^{i+1}}{i!} + \frac{h^\alpha}{\Gamma(\alpha+2)} \psi_3(t_{n+1}, I_2^p(t_{n+1})) + \frac{h^\alpha}{\Gamma(\alpha+2)} \sum_{j=0}^{n} \lambda_{j,n+1} \psi_3(t_j, I_2(t_j)), \\ R(t_{n+1}) = \sum_{i=0}^{\lceil\alpha\rceil-1} R_0^{(i)} \frac{t_{n+1}^{i+1}}{i!} + \frac{h^\alpha}{\Gamma(\alpha+2)} \psi_4(t_{n+1}, R^p(t_{n+1})) + \frac{h^\alpha}{\Gamma(\alpha+2)} \sum_{j=0}^{n} \lambda_{j,n+1} \psi_4(t_j, R(t_j)), \end{cases}$$

$$\begin{cases} S^p(t_{n+1}) = \sum_{i=0}^{\lceil\alpha\rceil-1} S_0^{(i)} \frac{t_{n+1}^{i+1}}{i!} + \frac{1}{\Gamma(\alpha)} \sum_{k=0}^{n} \Lambda_{k,n+1} \psi_1(t_k, S(t_k)), \\ I_1^p(t_{n+1}) = \sum_{i=0}^{\lceil\alpha\rceil-1} I_{1,0}^{(i)} \frac{t_{n+1}^{i+1}}{i!} + \frac{1}{\Gamma(\alpha)} \sum_{k=0}^{n} \Lambda_{k,n+1} \psi_2(t_k, I_1(t_k)), \\ I_2^p(t_{n+1}) = \sum_{i=0}^{\lceil\alpha\rceil-1} I_{2,0}^{(i)} \frac{t_{n+1}^{i+1}}{i!} + \frac{1}{\Gamma(\alpha)} \sum_{k=0}^{n} \Lambda_{k,n+1} \psi_3(t_k, I_2(t_k)), \\ R^p(t_{n+1}) = \sum_{i=0}^{\lceil\alpha\rceil-1} R_0^{(i)} \frac{t_{n+1}^{i+1}}{i!} + \frac{1}{\Gamma(\alpha)} \sum_{k=0}^{n} \Lambda_{k,n+1} \psi_4(t_k, R(t_k)), \end{cases}$$

where

$$\lambda_{j,n+1} = \begin{cases} n^{\alpha+1} - (n-\alpha)(n+1)^\alpha, & j = 0, \\ (n-j+2)^{\alpha+1} + (n-j)^{\alpha+1} - 2(n-j+1)^{\alpha+1}, & 1 \leqslant j \leqslant n, \\ 1, & j = n+1, \end{cases}$$

and

$$\Lambda_{k,n+1} = \frac{h^\alpha}{\alpha}((n+1-k)^\alpha - (n-k)^\alpha).$$

The proposed technique is fully explained by the authors in [3]. Using MATLAB 16, we demonstrate the numerical simulation of the suggested model based on the predictor-corrector (PECE) method of ABM. The initial values for the states are as follows: $S_0 = 0.99, I_{1,0} = 0.1, I_{2,0} = 0.2, R_0 = 0.3$. The bifurcation diagrams are employed to investigate the influences of key parameters on the state variables. Using the values of parameters shown in Table 2, the bifurcation diagrams are obtained in Figure 4. It is clear that increasing the rate of resistance evolution tends to induce oscillatory dynamics of state variables. Also, it is found that increasing the value of b_7^α suppresses these observed oscillations. Where $\alpha = 1$, we obtained the bifurcation diagrams in Figure 4.

Table 2: The first set of values of parameters for model (3.2).

Parameter	Value
b_1^α	$(0.2)^\alpha$
b_2^α	$(0.04)^\alpha$
b_3^α	$(0.4)^\alpha$
b_4^α	$(0.04)^\alpha$
b_5^α	$(0.03)^\alpha$
b_6^α	$(0.5)^\alpha$
b_7^α	$(0.03)^\alpha$
p	$(1)^\alpha$

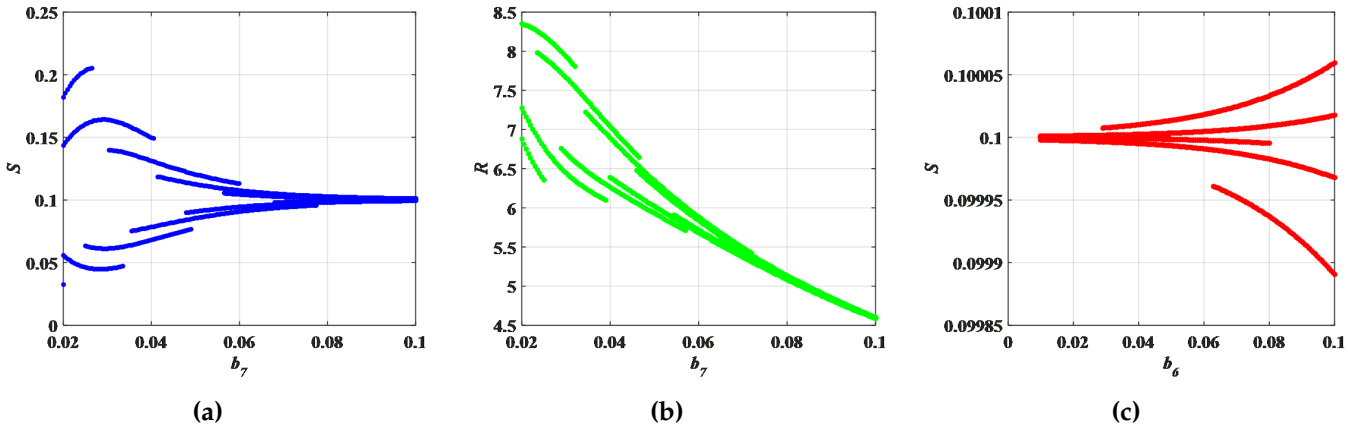

Figure 4: Bifurcation diagrams of S and R with respect to b_6 and b_7.

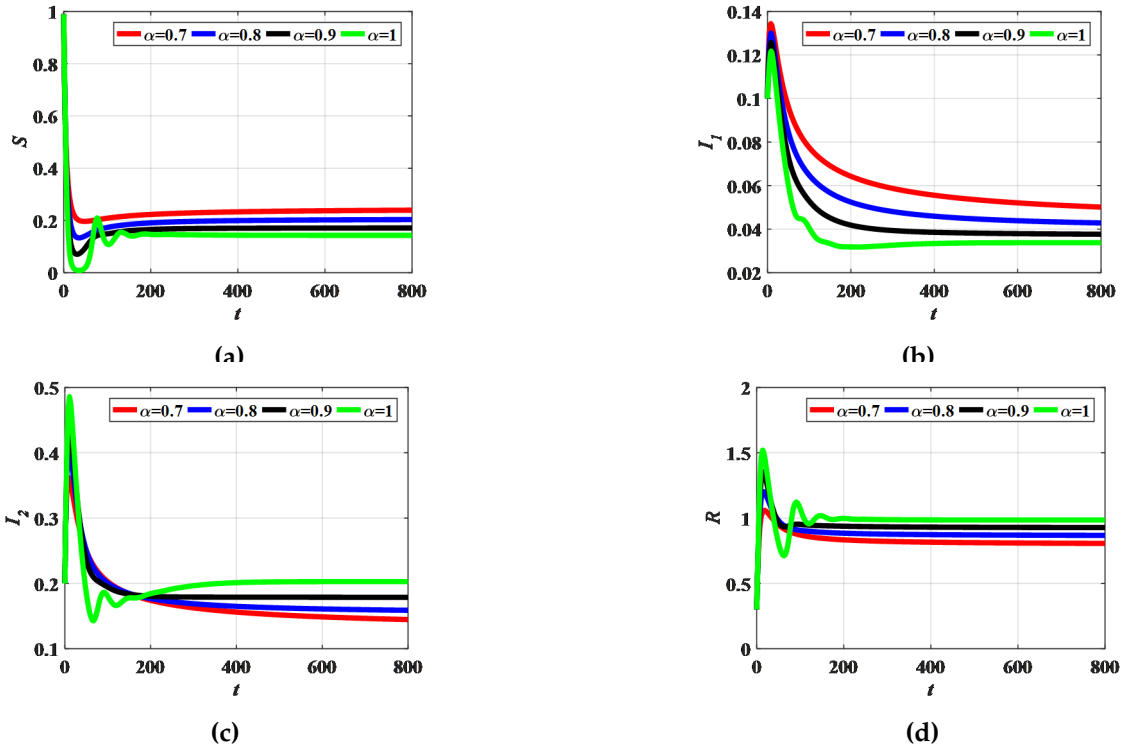

Figure 5: Solution profiles of the different compartments for $\alpha = 1,\ 0.9,\ 0.8,\ 0.7$ using the PECE method of ABM.

The second set of values of parameters for model (3.2) are given in Table 3. Figure 5 shows the numerical solutions for the proposed model at α = 0.7, 0.8, 0.9, 1. Figure 5 illustrates the result of the fractional term's addition. The effect of the fractional order is clear as S, $I_1(t)$, and $I_2(t)$ states are decreased gradually while R increases. Also, it can be depicted that while changing the value of α the states become more stable for fewer values of α which indicates the success of the proposed problem of modeling the antimicrobial resistance. The phase portraits between the different compartments are shown in Figure 6. Additionally, Figure 7 displays a 3D plot of states versus time and fractional order α along with the associated contour plot. Figures 6 and 7 provide a detailed presentation of the results achieved through the inclusion of the fractional term in the analysis. The influence of the fractional order becomes distinctly visible as the susceptible S and infected states ($I_1(t)$, $I_2(t)$) demonstrate a gradual decrease in their respective magnitudes, with a simultaneous increase observed in the R state. Additionally, it becomes apparent that the variations in the parameter α lead to a notable enhancement in the stability of the states within a narrower spectrum of α values. This observation underscores the effectiveness and

precision of the proposed methodology in the modeling of antimicrobial resistance dynamics. Where $\alpha = 1$, we obtained the bifurcation diagrams in Figure 5.

Table 3: The second set of values of parameters for model (3.2).

Parameter	Value
b_1^α	$(0.2)^\alpha$
b_2^α	$(0.3)^\alpha$
b_3^α	$(0.4)^\alpha$
b_4^α	$(0.02)^\alpha$
b_5^α	$(0.03)^\alpha$
b_6^α	$(0.5)^\alpha$
b_7^α	$(0.06)^\alpha$
p	$(0.1)^\alpha$

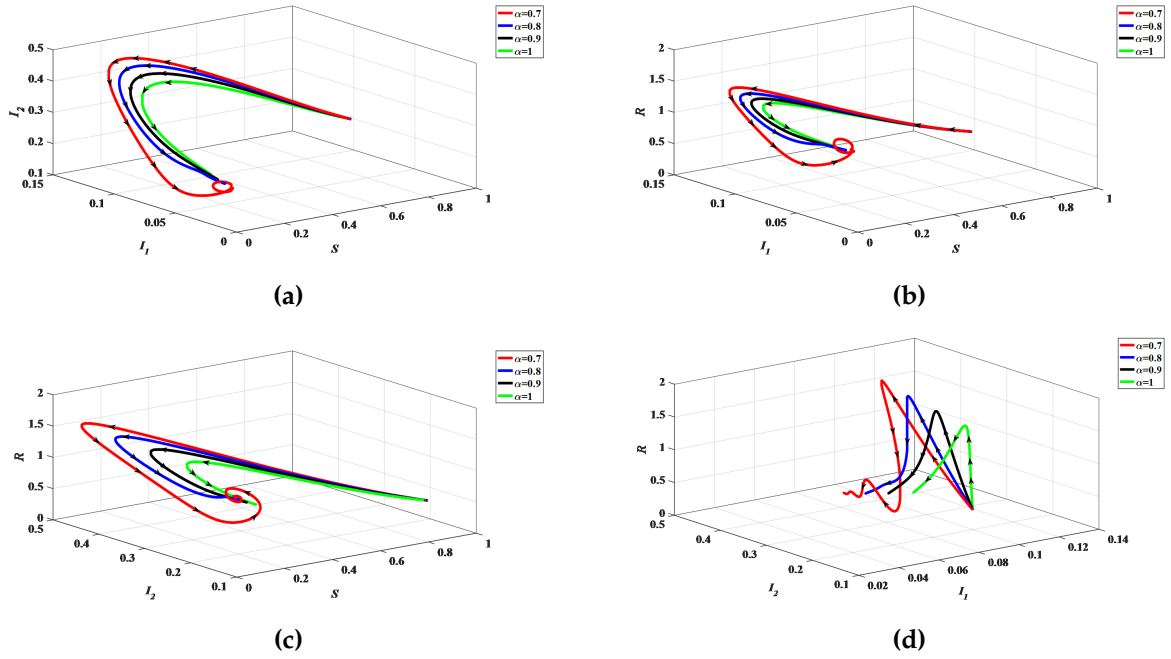

Figure 6: Phase portraits of the different compartments of the model (3.2).

The occurrence of Hopf bifurcation is investigated in parameters space of the model via defining the function Δ as follows

$$\Delta = Arg\,(\lambda_i) - \frac{\alpha\pi}{2}.$$

Then the changes in Δ are tracked in the space of parameters to determine the critical bifurcation values at which the value of Δ transversally passes through the value of 0. Thorough numerical investigations depict that Hopf bifurcation does not exist in the model. Figures 8-11 show the results of the second scenario of simulation experiments. In this case, the model exhibits decaying oscillatory dynamics in its phase space at the values of parameters given in Table 4. Figure 8 shows the numerical solutions for the proposed model at α = 0.7, 0.8, 0.9, 1. Figure 8 illustrates the effect of the fractional order, it is clear that S, $I_1(t)$, and $I_2(t)$ states are decreased gradually while R increases. Also, it can be depicted that while changing the value of α the states become more stable for the small values of α. The 3D phase portraits between the different compartments are shown in Figure 9. Figure 9 shows that the oscillation increases as the fractional order α increases. The 2D phase portraits between the different compartments are shown in

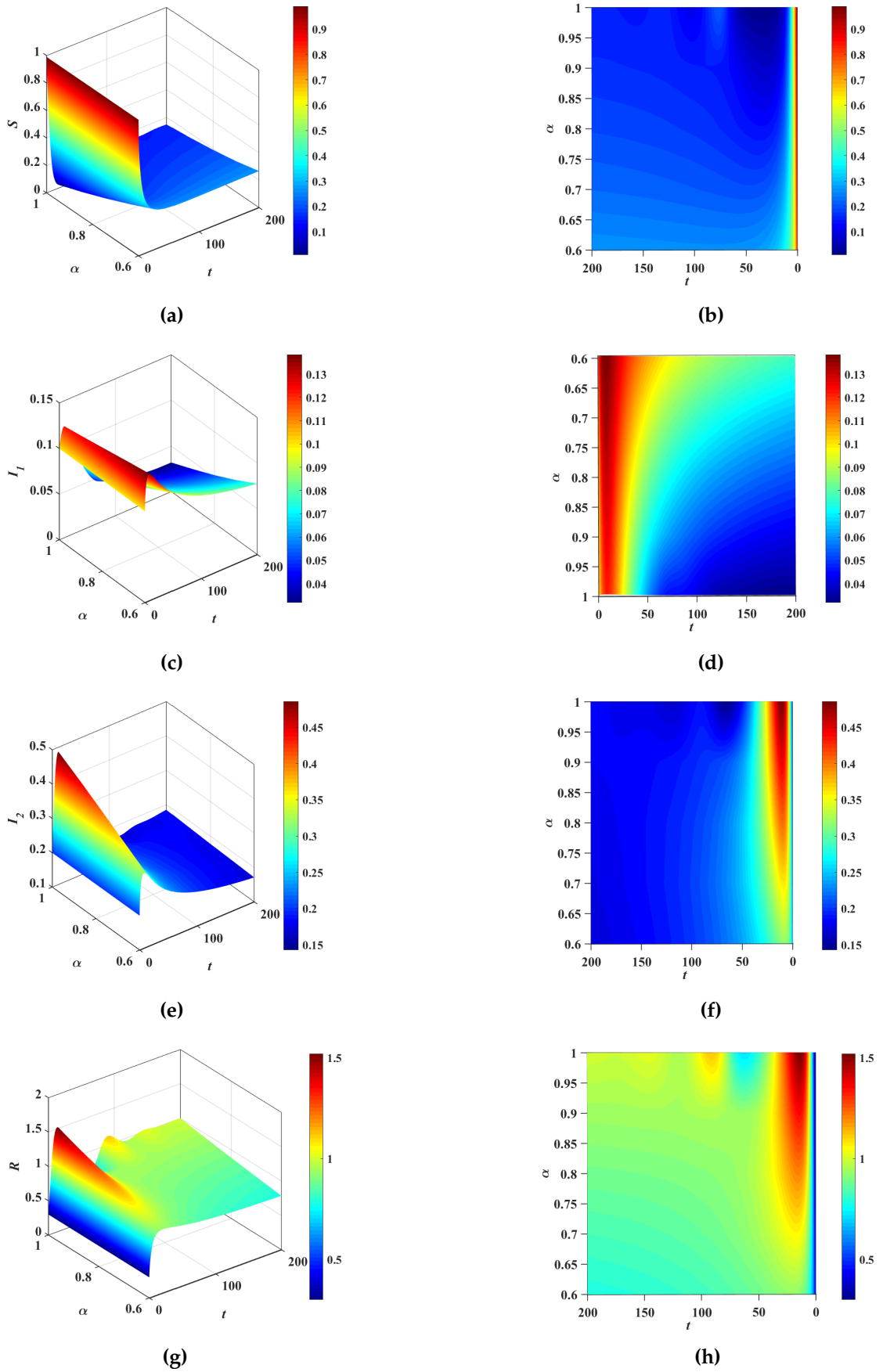

Figure 7: 3D plots of the compartments populations versus time and fractional order α with the corresponding contour plots.

Figure 10. Also, it is clear from Figure 10 that the oscillation increases as the fractional order α increases. Finally, Figure 11 displays a 3D plot of states versus time and fractional order α along with the associated contour plot. In Figure 11, the states become more stable as the time increases and the fractional order decreases.

Table 4: The third set of values of parameters for model (3.2).

Parameter	Value
b_1^α	$(0.2)^\alpha$
b_2^α	$(0.04)^\alpha$
b_3^α	$(0.4)^\alpha$
b_4^α	$(0.02)^\alpha$
b_5^α	$(0.03)^\alpha$
b_6^α	$(0.5)^\alpha$
b_7^α	$(0.03)^\alpha$
p	$(1)^\alpha$

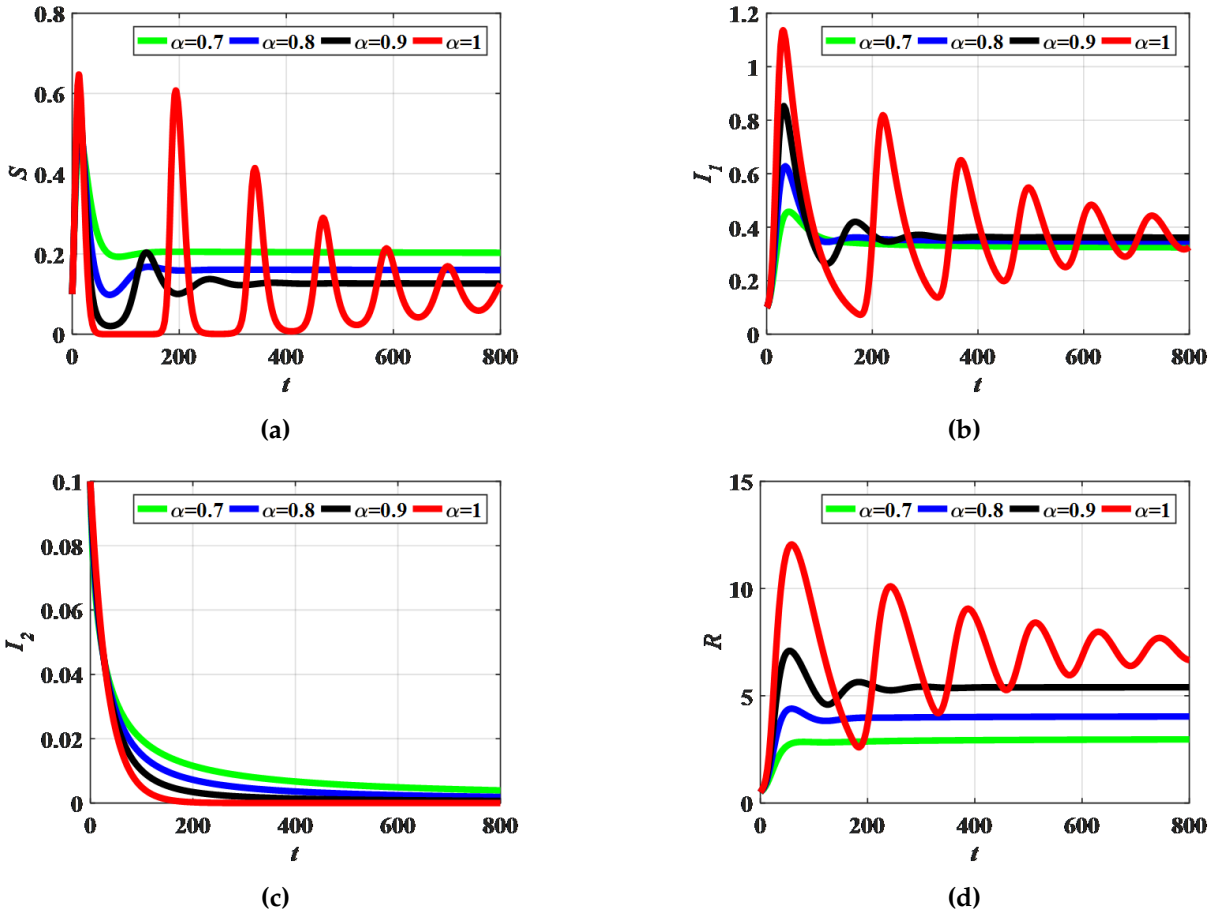

Figure 8: Solution profiles of the different compartments for $\alpha = 1,\ 0.9,\ 0.8,\ 0.7$ using the PECE method of ABM for the values of parameters in Table 4.

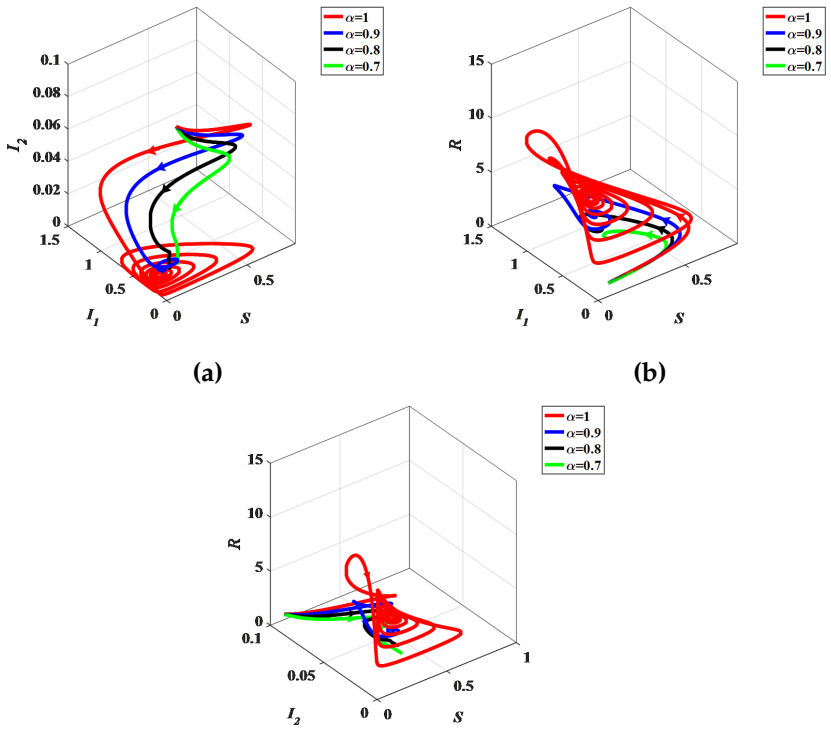

Figure 9: 3D Phase portraits of the different compartments of the model (3.2) for the values of parameters in Table 4.

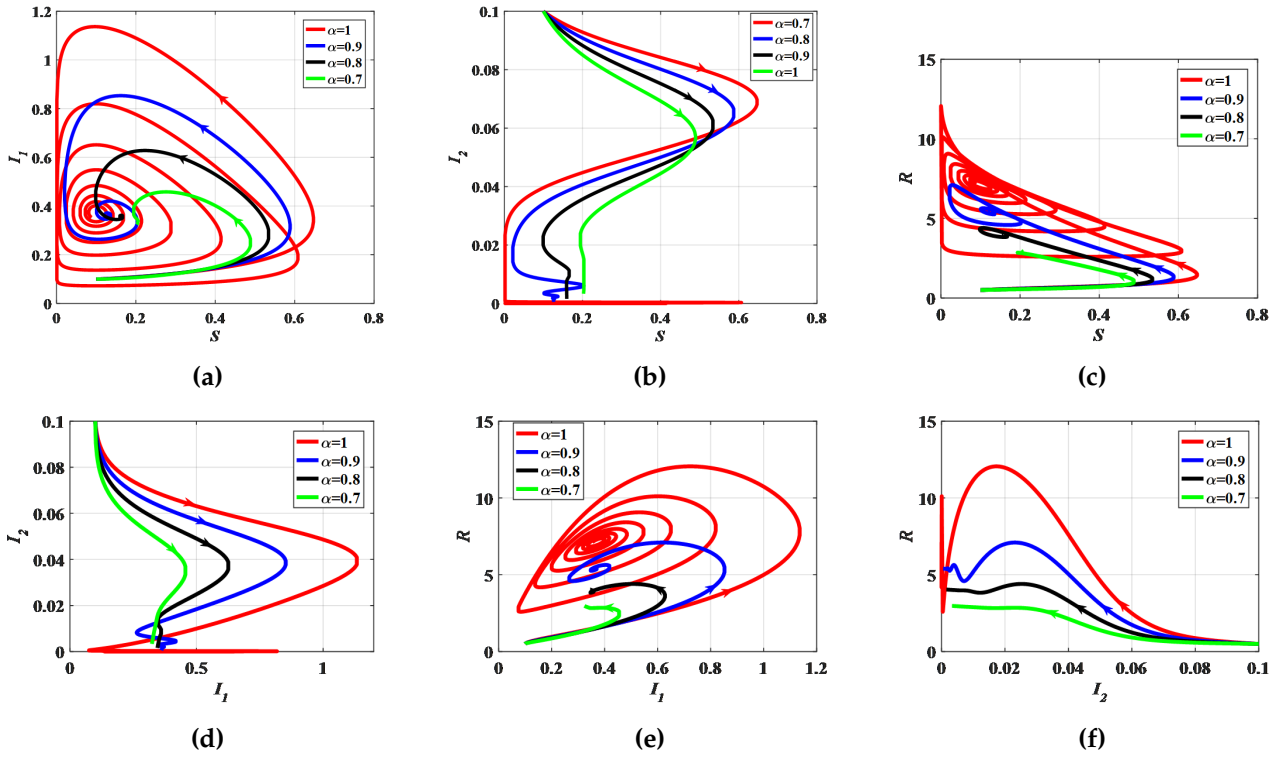

Figure 10: Phase portraits of the different compartments of the model (3.2) for the values of parameters in Table 4.

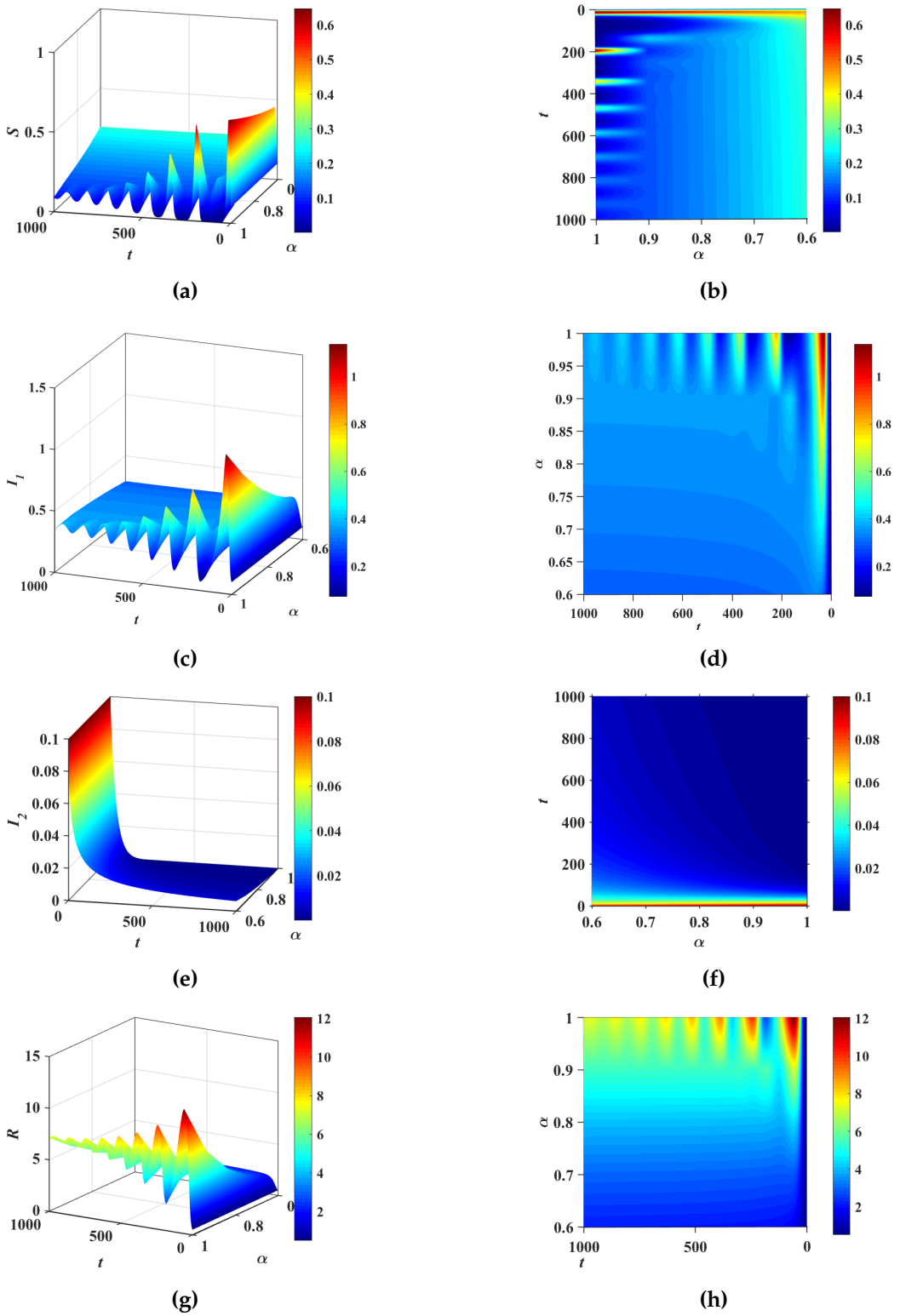

Figure 11: 3D plots of the compartments populations versus time and fractional order α with the corresponding contour plots for the values of parameters in Table 4.

6. Conclusion

The dynamics of a proposed fractional order antibiotic resistance model are explored in this study. It is depicted that the present model has four steady states. One of the steady states of the model is

always unstable. The stability of the remaining steady states is affected by key parameters in the model along with the value of fractional order which reflects memory influence. In particular, the stability of disease-free equilibrium point is E_2 requires that $b_2^\alpha < b_7^\alpha$ and $b_1^\alpha \left(b_4^\alpha + p^\alpha b_5^\alpha\right) < b_4^\alpha b_5^\alpha + p^\alpha b_4^\alpha b_1^\alpha$. In other words, the infection rate of resistant strains should be sufficiently reduced via suitable control and health-care measures. Also, the of rate treatment with antibiotics should be kept at minimum accurate and necessary dose to maintain stability of healthy steady state. Stability regions are obtained in the space of parameters of model (3.2) for the coexistence equilibrium point. It is found that stability region in $b_1 - b_2$ space shrinks when the value of discharge rate for infected individuals with resistant strains is increased. The equilibrium point E_4 are observed to lose its stability for small values of infection rate of sensitive strains and relatively moderate to large values of b_2. It is demonstrated that the fractional order model does not exhibit the Hopf bifurcation in the way that the possible oscillatory dynamics of the model are decaying with time. From another perspective, the memory effects introduced by fractional-order derivatives have been observed to mitigate the oscillatory dynamics seen in the model's phase space. The theoretical analysis is validated through numerical simulations. The key recommendations stemming from this study include: precise administration of antibiotic dosages, governmental efforts to control all forms of pollution, and increased investments in research for new types of antibiotics and infection control in healthcare facilities. Prioritizing appropriate antibiotic treatments is essential for effectively addressing this issue in the future. Our view is that a thorough examination of upcoming research suggests that utilizing multi-antibiotic therapy presents a more effective and efficient approach compared to solely relying on single antibiotic treatments to combat the challenge of antibiotic resistance.

Author contributions

AAE: conceptualization, investigation, visualization, reviewing, editing, finalizing this paper, funding supervision, and writing-original draft.

AE: conceptualization, data acquisition, investigation, analysis, interpretation of data, and writing-original draft.

Funding

This study is supported via funding from Prince Sattam bin Abdulaziz University project number (PSAU/2023/01/25741).

Data availability

All data generated or analyzed during this study are included in this article.

Human participants and/or animals

This article does not contain any studies with human participants or animals performed by any of the authors.

Acknowledgements

The authors extend their appreciation to Prince Sattam bin Abdulaziz University for funding this research work through the project number (PSAU/2023/01/25741).

References

[1] H. Abboubakar, L. K. Kombou, A. D. Koko, H. P. E. Fouda, A. Kumar, *Projections and fractional dynamics of the typhoid fever: a case study of Mbandjock in the Centre Region of Cameroon*, Chaos Solitons Fractals, **150** (2021), 24 pages. 3.1, 5

[2] Access to Medicine Foundation, *2012 Access to Medicine Index*, (2012). 1

[3] E. Ahmed, A. S. Elgazzar, A. A. Elsadany, *Simple mathematical models of antimicrobial resistance*, J. Fract. Calc. Appl., **11** (2020), 22–25. 3, 3, 5

[4] E. Ahmed, A. E. Matouk, *Complex dynamics of some models of antimicrobial resistance on complex networks*, Math. Methods Appl. Sci., **44** (2021), 1896–1912. 1

[5] H. A. Antosiewicz, J. K. Hale, *Studies in ordinary differential equations*, Mathematical Association of America, California, (1977). 3.1

[6] F. Brauer, C. Castillo-Chavez, *Mathematical models in population biology and epidemiology*, Springer, New York, (2012). 1

[7] J. C. Butcher, *Numerical methods for ordinary differential equations in the 20th century*, J. Comput. Appl. Math., **125** (2000), 1–29. 5

[8] B. Daşbaşı, *Fractional order bacterial infection model with effects of anti-virulence drug and antibiotic*, Chaos Solitons Fractals, **170** (2023), 17 pages. 1

[9] B. Daşbaşı, I. Öztürk, *Mathematical modelling of bacterial resistance to multiple antibiotics and immune system response*, SpringerPlus, **5** (2016), 1–17. 1

[10] O. Diekmann, K. Dietz, J. Heesterbeek, *The basic reproduction ratio for sexually transmitted diseases: I. theoretical considerations*, Math. Biosci., **107** (1991), 325–339. 4

[11] K. Diethelm, *The analysis of fractional differential equations*, Springer-Verlag, Berlin, (2004). 2, 3

[12] K. Diethelm, N. J. Ford, A. D. Freed, *A predictor-corrector approach for the numerical solution of fractional differential equations*, Nonlinear Dynam., **29** (2002), 3–22. 5

[13] M. F. Elettreby, E. Ahmed, *Multi-drug antimicrobial resistance model*, Math. Methods Appl. Sci., **43** (2020), 10462–10473. 1

[14] M. F. Elettreby, A. S. Alqahtani, E. Ahmed, *Fractional-order model for multi-drug antimicrobial resistance*, Comput. Model. Eng. Sci., **124** (2020), 665–682. 1, 3

[15] M. F. Elettreby, A. S. Alqahtani, T. Nabil, *Complex dynamical behavior of a discretize fractional-order multi-drug antimicrobial resistance model*, Alex. Eng. J., **59** (2020), 3119–3131 1

[16] A. Elsonbaty, W. Adel, A. Aldurayhim, A. El-Mesady, *Mathematical modeling and analysis of a novel monkeypox virus spread integrating imperfect vaccination and nonlinear incidence rates*, Ain Shams Eng. J., **15** (2024), 19 pages. 1

[17] *European Centre for Disease Prevention and Control. ECDC/EMEA Joint Technical Report*, The Bacterial Challenge: Time to React., (2009). 1

[18] A. Frei, A. D. Verderosa, A. G. Elliott, J. Zuegg, M. A. T. Blaskovich, *Metals to combat antimicrobial resistance*, Nat. Rev. Chem., **7** (2023), 202–224. 1

[19] R. Garrappa, *Predictor-corrector PECE method for fractional differential equations*, MATLAB Central File Exchange, (2011). 5

[20] E. Ibargüen-Mondragón, S. Mosquera, M. Cerón, E. M. Burbano-Rosero, S. P. Hidalgo-Bonilla, L. Esteva, J. P. Romero-Leitón, *Mathematical modeling on bacterial resistance to multiple antibiotics caused by spontaneous mutations*, Biosystems, **117** (2014), 60–67. 1

[21] E. Ibargüen-Mondragón, J. P. Romero-Leiton, L. Esteva, E. M. Burbano-Rosero, *Mathematical modeling of bacterial resistance to antibiotics by mutations and plasmids*, J. Biol. Systems, **24** (2016), 129–146. 1

[22] E. M. Izhikevich, *Dynamical systems in neuroscience: the geometry of excitability and bursting*, MIT Press, Cambridge, MA, (2007). 1

[23] M. Kot, *Elements of mathematical ecology*, Cambridge University Press, Cambridge, (2001). 1

[24] J. P. LaSalle, *The stability of dynamical systems*, Society for Industrial and Applied Mathematics, Philadelphia, PA, (1976). 4

[25] J. A. Lewnard, Y. H. Grad, *Vaccine waning and mumps re-emergence in the United States*, Sci. Transl. Med., **10** (2018). 1

[26] C. Li, F. Zeng, *The finite difference methods for fractional ordinary differential equations*, Numer. Funct. Anal. Optim., **34** (2013), 149–179. 3.1

[27] W. Lin, *Global existence theory and chaos control of fractional differential equations*, J. Math Anal. Appl., **332** (2007), 709–726. 3.1

[28] E. Massad, M. N. Burattini, F. A. B. Coutinho, *An optimization model for antibiotic use*, Appl. Math. Comput., **201** (2008), 161–167. 1

[29] S. M. Moghadas, *Modelling the effect of imperfect vaccines on disease epidemiology*, Discrete Contin. Dyn. Syst. Ser. B, **4** (2004), 999–1012. 1

[30] T. Nguiwa, G. G. Kolaye, M. Justin, D. Moussa, G. Betchewe, A. Mohamadou, *Dynamic study of* SI_AI_SQVR-B *fractional-order cholera model with control strategies in Cameroon Far North Region*, Chaos Solitons Fractals, **144** (2021), 19 pages. 5

[31] Z. M. Odibat, N. T. Shawagfeh, *Generalized Taylor's formula*, Appl. Math. Comput., **186** (2007), 286–293. 3.1
[32] I. Petráš, *Fractional-order nonlinear systems: modeling, analysis and simulation*, Springer, London, (2011). 3.1, 4
[33] J. Pieskä, E. Laitinen, A. Lapin, *Predictor-corrector methods for solving continuous casting problem*, In: Domain decomposition methods in science and engineering, Springer, Berlin, **40** (2005), 677–684. 5
[34] M. A. Salam, M. Y. Al-Amin, M. T. Salam, J. S. Pawar, N. Akhter, A. A. Rabaan, M. A. A. Alqumber, *Antimicrobial resistance: a growing serious threat for global public health*, Healthcare, **11** (2023), 20 pages. 1
[35] S. M. Salman, R. Han, *Complex patterns in a space-time discrete mathematical model of antibiotic resistance in hospitals with self-diffusion*, Commun. Nonlinear Sci. Numer. Simul., **127** (2023), 23 pages. 1
[36] B. Sartorius, A. P. Gray, N. D. Weaver, G. R. Aguilar, L. R. Swetschinski, K. S. Ikuta, T. Mestrovic, E. Chung, E. E. Wool, C. Han, *The burden of bacterial antimicrobial resistance in the WHO African region in 2019: a cross-country systematic analysis*, Lancet Glob. Health, **12** (2024), E201–E216. 1
[37] P. D. Tamma, E. L. Heil, J. A. Justo, A. J. Mathers, M. J. Satlin, R. A. Bonomo, *Infectious Diseases Society of America 2023 guidance on the treatment of antimicrobial resistant gram-negative infections*, Clin. Infect. Dis., (2024), 56 pages. 1
[38] M. S. Tavazoei, M. Haeri, *Chaotic attractors in incommensurate fractional order systems*, Phys. D, **237** (2008), 2628–2637. 4
[39] L. Ternent, R. J. Dyson, A.-M. Krachler, S. Jabbari, *Bacterial fitness shapes the population dynamics of antibiotic-resistant and-susceptible bacteria in a model of combined antibiotic and anti-virulence treatment*, J. Theor. Biol., **372** (2015), 1–11. 1
[40] P. Van den Driessche, J. Watmough, *Reproduction numbers and sub-threshold endemic equilibria for compartmental models of disease transmission*, Math. Biosci., **180** (2002), 29–48. 4
[41] C. Vargas-De-León, *Constructions of Lyapunov functions for classics SIS, SIR and SIRS epidemic model with variable population size*, Foro-Red-Mat: Rev. Electrón. Conten. Mat., **26** (2009), 1–12. 5
[42] WHO, *Ten threats to global health in 2019*, (2019). 1
[43] WHO, *Antibiotic resistance*, (2023). 1